REMOTE SENS. ENVIRON. 32:111–124 (1990)

Spectral Estimates of Net Radiation and Soil Heat Flux

C. S. T. Daughtry
Remote Sensing Research Laboratory, Agricultural Research Service, USDA, Beltsville, Maryland

W. P. Kustas
Hydrology Laboratory, Agricultural Research Service, USDA, Beltsville, Maryland

M. S. Moran, P. J. Pinter, Jr., and R. D. Jackson
U.S. Water Conservation Laboratory, Agricultural Research Service, USDA, Phoenix

P. W. Brown
Department of Soil and Water Science, University of Arizona, Tucson

W. D. Nichols
Water Resources Division, U.S. Geological Survey, Carson City, Nevada

L. W. Gay
School of Renewal Resources, University of Arizona, Tucson

Location: University of Arizona Maricopa Agricultural Center (MAC)

$$R_n = LE + H + G,$$

The primary objective of our study was to estimate net radiation and soil heat flux using ground-based meteorological data and remotely sensed multispectral data acquired from an airplane at 150 m over irrigated agricultural fields. The estimates provide a means to evaluate the available energy of the surface ($R_n - G$), which can be partitioned to latent and sensible heat under nonadvective conditions. The remote estimates of G and R_n along flight lines in five fields were compared to point measurements of G and R_n from nine ground-based stations.

Evaluation of Radiation Terms

The net radiation equation [Eq. (2)] can be rewritten in the form

$$R_n = R_{Si} - R_{So} + e_a \sigma T_a^4 - e_s \sigma T_s^4, \qquad (3)$$

where e_a is the effective emissivity for a cloudless sky, σ is the Stefan–Boltzman constant, T_a is the air temperature (°K), e_s is surface emissivity, and T_s is the surface temperature (°K).

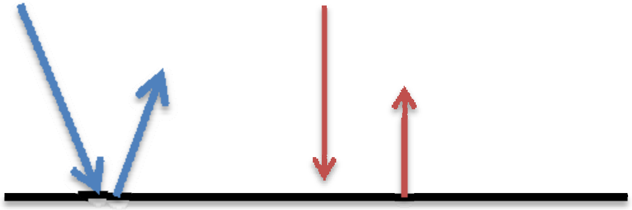

Agricultural field transects

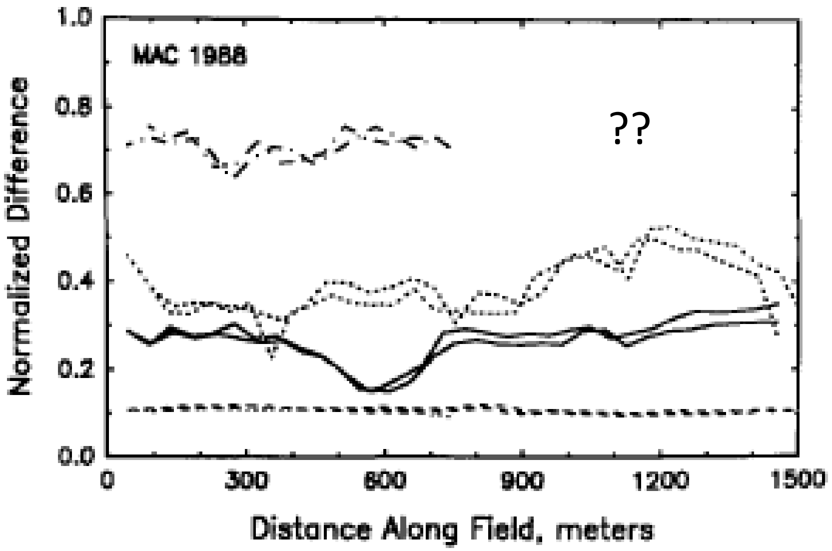

Figure 1. Values of the normalized difference vegetative index (NDVI) along transects through five fields. The multispectral data were acquired from an aircraft at 150 m by a radiometer with SPOT filters. The two transects along the center of each field were flown in opposite directions with mean times of data acquisition that coincided within 8 min of the SPOT satellite overpass on 11 June 1988. (–·–) Alfalfa 21; (—) Cotton 28; (- - -) Cotton 29; (– – –) Soil 32, smooth; (· · ·) Soil 27, rough.

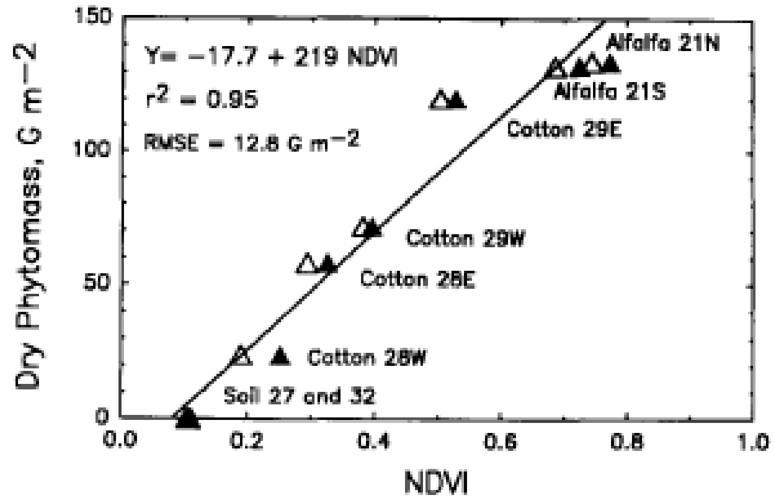

Figure 2. Relationship of total dry phytomass and normalized difference vegetative index (NDVI). The mean time of the aircraft overflight was 1141 and 1111 MST on 11 (△) and 12 (▲) June 1988, respectively.

Transects

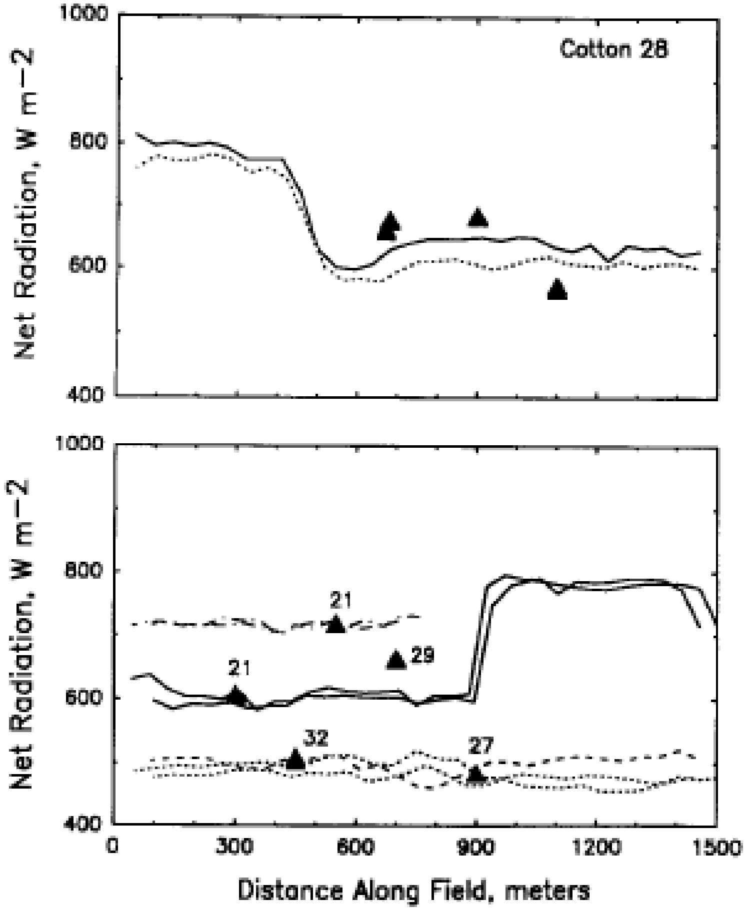

Figure 3. Values of remote net radiation (Brest-Goward + Satterlund formula) along transects through five fields on 11 June 1988. The triangles represent net radiation measured by ground stations in each field. Bottom: (–·–) Alfalfa 21; (—) Cotton 29; (– – –) Soil 27, rough; (- - -) Soil 32, smooth.

Field	*Location (m)*	*Station*
Cotton 28	670	1
	680	2
	900	3
	1100	4
Cotton 29	700	8
	700	8
Alfalfa 21	300	6
	550	5
Soil 27	900	7
Soil 32	450	9

Method for Calculating Soil Heat Flux

Soil heat flux (G) at the surface was estimated by a combination of soil calorimetry and measurement of the heat flux density at the depth given in Table 1 using heat flow plates (Fuchs and Tanner, 1966). Kustas and Daughtry (1990) describe in detail the procedures and corrections used to calculate soil heat flux for this experiment. Briefly, the changes in heat storage of the soil layer above the plate is added to the values measured by the soil heat flux plate. The volumetric heat capacity, estimated as a function of volume fractions of mineral soil, organic matter, and water (deVries, 1963), was assumed to be constant for the storage layer. Mean temperature of the soil layer above the soil heat flow plates was measured with thermocouples inserted into the soil between the heat flow plates and the soil surface (Table 1). Soil heat

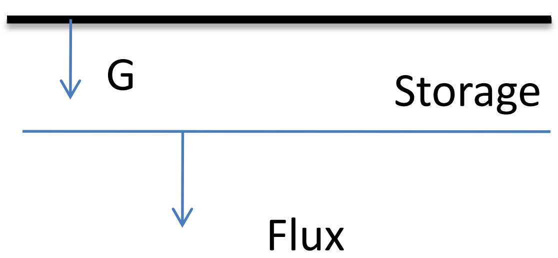

Compare Rn and G

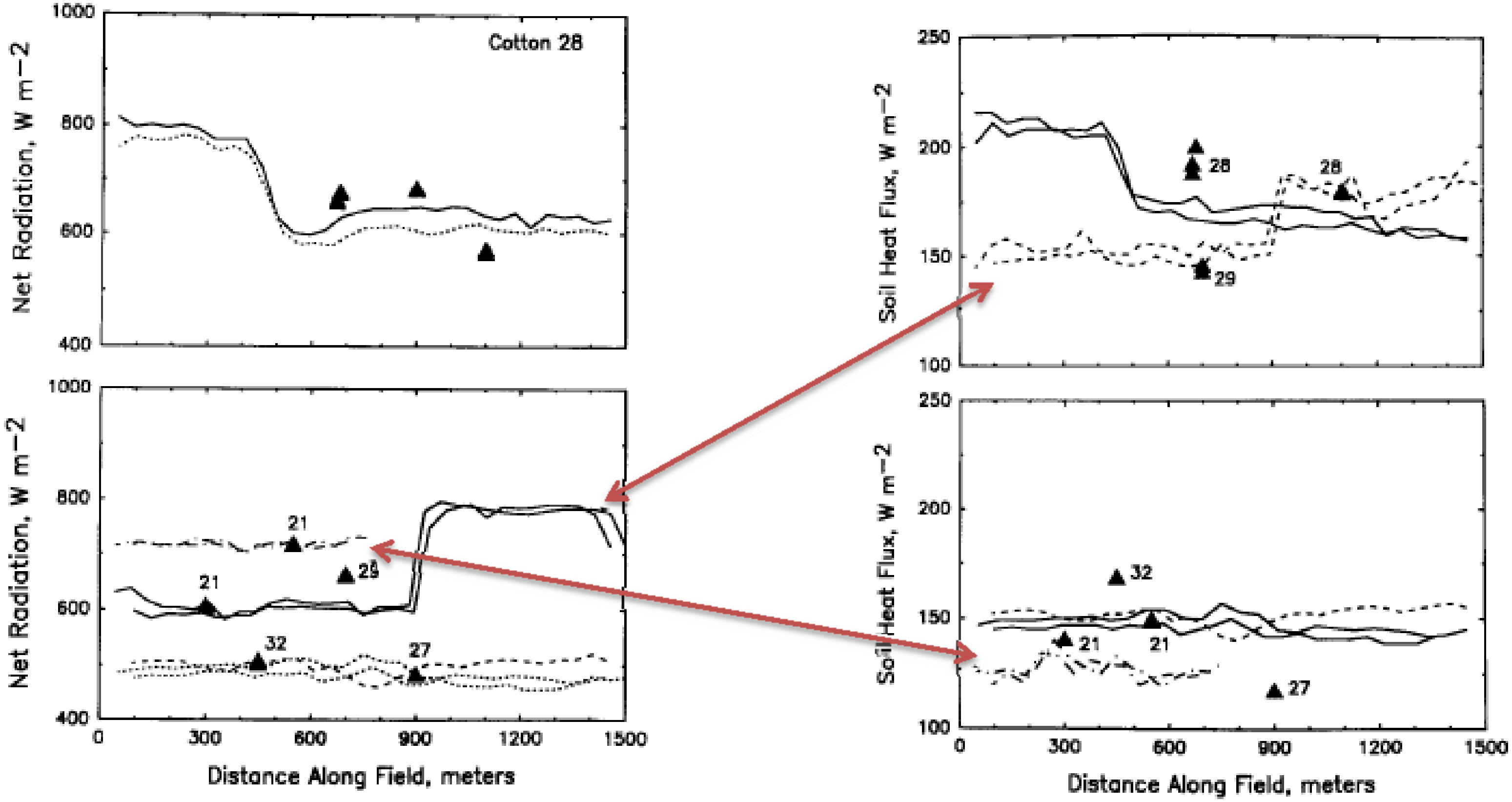

Figure 3. Values of remote net radiation (Brest-Goward + Satterlund formula) along transects through five fields on 11 June 1988. The triangles represent net radiation measured by ground stations in each field. Bottom: (–·–) Alfalfa 21; (—) Cotton 29; (– – –) Soil 27, rough; (---) Soil 32, smooth.

Figure 5. Values of remote soil heat flux ([$G = (0.325 - 0.208\ \mathrm{NDVI})R_n$], Kustas and Daughtry, 1990) along transects through five fields on 11 June 1988: (▲) soil heat flux measured by ground stations in each field. Top: (—) Cotton 28; (– – –) Cotton 29. Bottom (–·–) Alfalfa 21; (– – –) Soil 27, rough; (—) Soil 32, smooth.

Soil Heat Flux

Remote soil heat flux (remote G) was calculated as a function of remote R_n and the spectral vegetation indices using the following equations proposed by Clothier et al. (1986);

$$G = (0.295 - 0.0133\,\mathrm{IRRED})R_n, \qquad (9)$$

and Kustas and Daughtry (1990),

$$G = (0.294 - 0.0164\,\mathrm{IRRED})R_n \qquad (10)$$

$$G = (0.325 - 0.208\,\mathrm{NDVI})R_n \qquad (11)$$

where IRRED is the ratio of B3 and B2 reflectance factors and NDVI is the difference in reflectance factors between B3 and B2 divided by their sum. Tables 7 and 8 summarize the mean

Table 8. Mean Errors (e), Mean Absolute Errors ($|e|$), and Standard Deviations of Absolute Errors ($SD_{|e|}$) for Remote G Minus Measured G Data are Means of Eight Stations and Four Overflights on 11–12 June 1988 ($n = 31$, station 7 is missing for one flight on 11 June)[a]

Model[b]	e	$\|e\|$	$\|e\|$
		W/m^2	
Kustas (NDVI)	−3.2	19.7	17.5
Kustas (IRRED)	−2.2	21.8	17.7
Clothier (IRRED)	8.7	23.2	19.7
$0.1R_n$	−86.2	86.2	33.6
$0.2R_n$	−24.3	37.3	23.6
		(%)	
Kustas (NDVI)	2.2	13.3	11.8
Kustas (IRRED)	−1.5	14.7	12.0
Clothier (IRRED)	5.9	15.7	13.3
$0.1R_n$	−58.2	58.2	22.7
$0.2R_n$	−16.4	25.2	15.9

[a] Mean measured $G = 148$ W/m^2.

[b] Methods of estimating soil heat flux: Kustas = Kustas and Daughtry (1990); Clothier = Clothier et al. (1986).

Conclusions

1. Ground heat flux scales with Rn
2. G ranges from 5 to 50% of Rn
3. Rn and G can be determined from space
4. The ratio G/Rn decreases with NDVI as vegetation screens the soil from the direct solar beam

$$G = (0.325 - 0.208\,\mathrm{NDVI})R_n$$

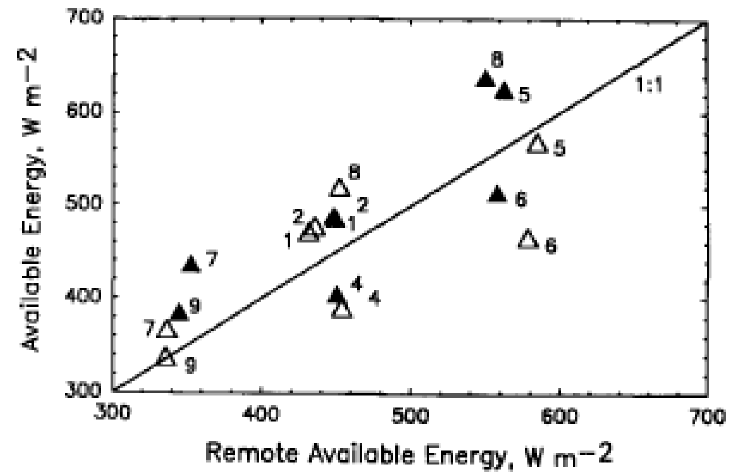

Figure 6. Values of measured available energy ($R_n - G$) versus values of remote available energy (remote R_n − remote G) for nine stations (Table 1) on 11 (△) and 12 (▲) June 1988.

Journal of Hydrology
Journal of Hydrology 212–213 (1998) 198–212

A remote sensing surface energy balance algorithm for land (SEBAL) 1. Formulation

W.G.M. Bastiaanssen[a,*], M. Menenti[a], R.A. Feddes[b], A.A.M. Holtslag[c]

$$\Gamma = \frac{G_0}{Q^*}$$

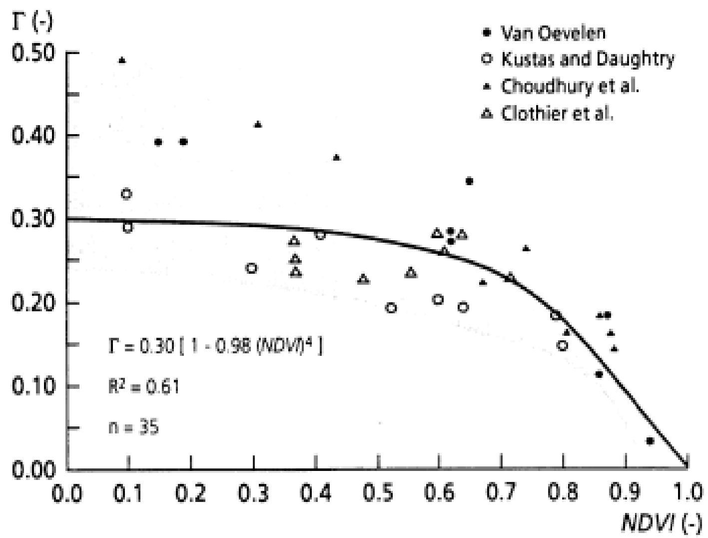

Fig. 3. Soil heat flux/net radiation data for a variety of surface types and soil cover as derived from Clothier et al. (1986), Choudhury (1989), Kustas and Daughtry (1990) and Van Oevelen (1993) to describe extinction effects by means of NDVI.